JACS
JOURNAL OF THE AMERICAN CHEMICAL SOCIETY
Communication
pubs.acs.org/JACS

Aqueous Lithium–Iodine Solar Flow Battery for the Simultaneous Conversion and Storage of Solar Energy

Mingzhe Yu, William D. McCulloch, Damian R. Beauchamp, Zhongjie Huang, Xiaodi Ren, and Yiying Wu*

Department of Chemistry & Biochemistry, The Ohio State University, 100 West 18th Avenue, Columbus, Ohio 43210, United States

Supporting Information

ABSTRACT: Integrating both photoelectric-conversion and energy-storage functions into one device allows for the more efficient solar energy usage. Here we demonstrate the concept of an aqueous lithium–iodine (Li–I) solar flow battery (SFB) by incorporation of a built-in dye-sensitized TiO_2 photoelectrode in a Li–I redox flow battery via linkage of an I_3^-/I^- based catholyte, for the simultaneous conversion and storage of solar energy. During the photoassisted charging process, I^- ions are photoelectrochemically oxidized to I_3^-, harvesting solar energy and storing it as chemical energy. The Li–I SFB can be charged at a voltage of 2.90 V under 1 sun AM 1.5 illumination, which is lower than its discharging voltage of 3.30 V. The charging voltage reduction translates to energy savings of close to 20% compared to conventional Li–I batteries. This concept also serves as a guiding design that can be extended to other metal-redox flow battery systems.

Simultaneous conversion and storage of solar energy marks a significant advance toward practical solar energy usage. Various kinds of solar fuels have been actively explored.[1] However, challenges with hydrogen storage and the cost of fuel cells make those systems complicated and difficult for implementation. A promising solution is integrating a photoelectrode into an electrochemical capacitor or battery to form a single device.[2] Several groups have made pioneering contributions toward this goal. For instance, the integration of dye-sensitized photoelectrochemical cells with redox flow batteries has been explored.[3] Our group has also demonstrated photo-assisted charging of a Li–O_2 battery.[2d] However, these devices are limited because they use organic solvents for the electrolyte. Besides the cost and the negative environmental impact of organic solvents, these systems cannot be incorporated with current aqueous redox flow battery systems because of their incompatible organic-solvent design. Recently, attempts at creating aqueous systems have been made by replacing the dye-sensitized photoelectrode with semiconductor photoelectrodes that have hydrophilic surfaces.[4] However, due to the semiconductors' large band-gap (i.e., 2.7 eV for WO_3 and 3.2 eV for TiO_2), these devices can only harvest a very limited portion of the solar spectrum (i.e., <460 nm).

Here, we report an aqueous lithium–iodine (Li–I) solar flow battery (SFB), a single device that integrates a Li–I redox flow battery[5] and a dye-sensitized solar cell (DSC)[6] via a linkage of I_3^-/I^- catholyte for simultaneous conversion and storage of solar energy. Using solar energy enables the Li–I SFB to be charged at an input voltage of 2.90 V under 1 sun 1.5 AM illumination and discharged at an output voltage of 3.30 V (at the current density of 0.50 mA cm^{-2}). Compared to conventional Li–I batteries, which are typically charged at a voltage over 3.60 V, the Li–I SFB can achieve energy savings up to 20% because of its voltage reduction. Furthermore, we have also proved with our example of the sodium–iodine (Na–I) SFB that this SFB concept can be extended to other metal–redox solar flow batteries.

The Li–I SFB has a three-electrode configuration (Figure 1a): a metallic Li anode, a Pt counter electrode (CE) and a dye-sensitized TiO_2 photoelectrode (PE). Both the CE and PE are in contact with the flowing I_3^-/I^- redox catholyte, which is stored in a reservoir connected to the catholyte chamber and pumped through the device using a peristaltic pump. The Li anode and I_3^-/I^- catholyte are separated by a piece of ceramic Li-ion

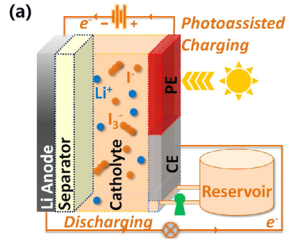

Figure 1. (a) Schematic of a Li–I SFB device with the three-electrode configuration; (b) energy diagram for the photoassisted charging process; (c) photoelectrochemical half-reactions.

Received: April 7, 2015
Published: June 23, 2015

DOI: 10.1021/jacs.5b03626
J. Am. Chem. Soc. 2015, 137, 8332–8335

conductive membrane, which allows for different solvents on each side. The discharging process is similar to that of conventional Li−I batteries: electrochemical oxidation of Li to Li^+ on the anode side and reduction of I_3^- to I^- on the CE side gives electricity output. However, the proposed charging process is different (Figure 1b): Here the external voltage is applied on the Li anode and the dye-sensitized TiO_2 PE. Upon illumination, dye molecules, which are chemically adsorbed on the TiO_2 semiconductor surface, get photoexcited and inject electrons into the conduction band of TiO_2 (steps 1 and 2 in Figure 1c). The oxidation of I^- to I_3^- then takes place by regenerating oxidized dye molecules (step 3 in Figure 1c). Meanwhile, Li^+ ions pass through the ceramic membrane and are reduced to metallic Li on the anode side (step 4 in Figure 1c), completing the full charging process.

The proposed mechanism indicates that the photoassisted charging voltage should equal the energy difference between the Li^+/Li redox potential and the quasi-Fermi level (E_f) of electrons in the TiO_2 semiconductor (which is at best close to the TiO_2 conduction band minimum, CBM) (Figure 1b). Since the CBM of TiO_2 lies at a more negative position than the I_3^-/I^- redox potential, the charging voltage of the Li−I SFB is expected to be smaller than that of conventional Li−I batteries, which is the redox potential difference between the Li^+/Li and I_3^-/I^- couples. The photoassisted charging process allows dye molecules to capture solar energy and then "pump" electrons from a lower energy level (i.e., the I_3^-/I^-redox potential) to a higher energy level (i.e., E_f of electrons in the TiO_2). Thus, a reduction of the charging voltage is expected.

The redox catholyte is the key component of this solar battery design because it bridges the Li−I battery and DSC components. Therefore, it is essential to confirm that a given catholyte recipe will work efficiently for both the battery and the solar cell. We started by investigating the Li−I battery and solar cell individually. We used the catholyte recipe of 2.00 M LiI, 0.05 M I_2, and 0.50 M guanidine thiocyanate (GuSCN) in saturated chenodeoxycholic acid (Cheno) aqueous solution (experimental details can be found in the Supporting Information (SI)). The LiI and I_2 provide ionic I^- and I_3^- species in the catholyte,[5b] while the GuSCN and Cheno additives facilitate the surface-wetting between the hydrophilic electrolyte and the hydrophobic dye-sensitized TiO_2 surface.[7] Cyclic voltammetry (CV) measurements (Figure S1) reveal that the addition of GuSCN and Cheno does not yield electrochemical side reactions for the battery operation within the working voltage window of 2.6−4.0 V (vs Li^+/Li; all potentials are referenced to the Li^+/Li redox in this communication).

A Li−I battery was fabricated and tested with the aforementioned electrolyte. It showed an average discharging voltage of 3.35 V and charging voltage of 3.55 V at a current density of 0.50 mA cm^{-2} (Figure 2). This matches well with the reported redox potential of I_3^-/I^- couple in water (i.e., ~3.5 V).[8] Compared to other Li-based batteries, the overpotential presented here is small (ca. 0.2 V), owing to the fast redox kinetics of I_3^-/I^- couple and the efficient solute diffusion in solution-phase electrolyte.[9]

The same aqueous electrolyte recipe was then used to fabricate a DSC with Z907 dye-sensitized TiO_2 film (dye molecular structure shown in Figure S2) on fluorine doped tin oxide (FTO) glass as the PE and platinum-coated FTO glass as the CE.[7] The addition of GuSCN and Cheno in the electrolyte efficiently disrupts the hydrogen bonding network between water molecules and facilitates electrolyte diffusion into the photo-

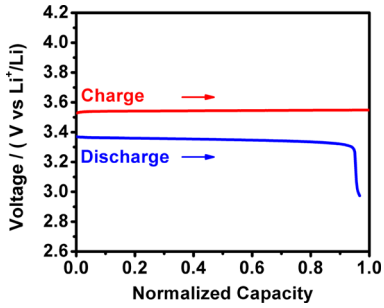

Figure 2. Typical charge−discharge profile of a conventional aqueous Li−I battery at a current density of 0.50 mA cm^{-2}. The voltage drop at the end of discharging process is due to the depletion of I_3^- ions in the catholyte.

electrode's mesoporous structure. Therefore, our aqueous electrolyte has excellent surface-wetting on the dye-sensitized TiO_2 photoelectrode surface. Under 1 sun 1.5 AM illumination, the solar cell's photocurrent−voltage (J−V) curve demonstrates that such a dye-sensitized TiO_2 PE is capable of generating a photovoltage of 0.50 ± 0.02 V at the working current of 0.50 mA cm^{-2} based on the average of four cells (Figure 3). The dye-

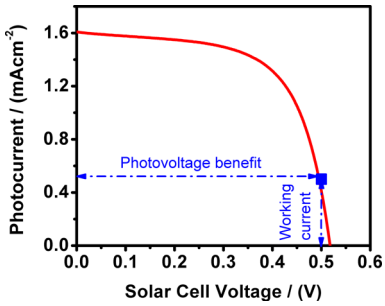

Figure 3. Typical J−V curve of an aqueous DSC under 1 sun 1.5 AM conditions. The blue spot indicates the photovoltage that is produced when working at a current density of 0.50 mA cm^{-2}.

regeneration process (step 3 in Figure 1c) is also kinetically favored, as it is an "in situ" process with the time constant on the microsecond scale.[10] Therefore, the dye-sensitized photoelectrode demonstrates efficient performance with the aqueous electrolyte for the photoelectrochemical production of I_3^- from I^-.

Given the excellent individual performance of both the Li−I battery and DSC with a common electrolyte, the as-conceived Li−I SFB was then constructed. Figure 4a shows the "light-response" feature of this device: during the charging process, the applied voltage decreases immediately once light is switched on,

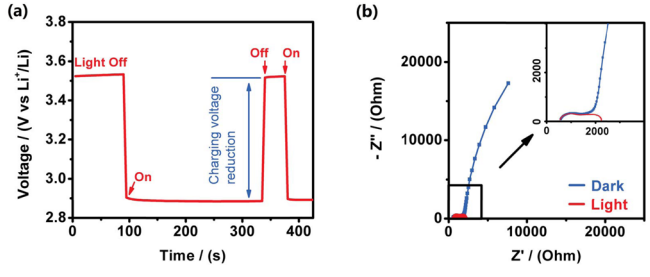

Figure 4. Light response of the Li−I SFB: (a) the charging voltage and (b) the EIS (OCV condition, 0.1 MHz to 1 Hz).

DOI: 10.1021/jacs.5b03626
J. Am. Chem. Soc. 2015, 137, 8332−8335

indicating that a photovoltage, which compensates for the cell's charging voltage, is generated on the PE. Once the light is turned off, the charging voltage increases instantly. The light response can also be seen in the Nyquist plots (Figure 4b), which were obtained through electrochemical impedance spectroscopy (EIS). The semicircle at low frequency is attributed to the recombination charge-transfer process at the PE−catholyte interface. Under illumination, the high electron concentration in the TiO_2 conduction band and sub-bandgap trap states induces a much smaller charge-transfer resistance. Because the E_f drops in the dark, the TiO_2 becomes more insulating and the recombination mainly occurs through the FTO−catholyte interface.[11]

The comparison between the charging profile of a conventional Li−I battery and the Li−I SFB is shown in Figure 5. Under

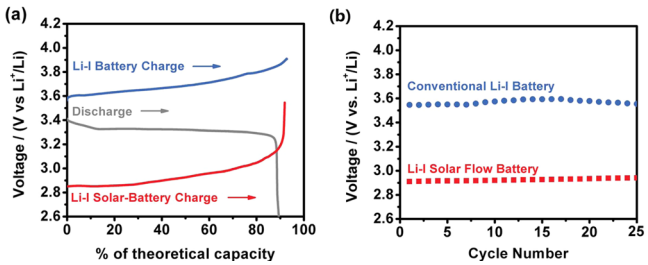

Figure 5. Performance comparison between Li−I SFB and conventional Li−I batteries: (a) a typical depleted charging and discharging voltage profile; (b) the initial charging voltages for 25 cycles.

1 sun 1.5 AM illumination, the Li−I SFB has an initial charging voltage of 2.90 ± 0.01 V at a current density of 0.50 mA cm^{-2} based on the average of three devices (Figure 5a). This value matches well with theoretical predictions, considering the energy gap between the TiO_2 CBM (i.e., +2.7 V at pH = 4.6, the pH of aqueous catholyte) and the E_f of electrons at working condition as well as the electrolyte-dye recombination and the device's internal series resistance. Compared to the conventional Li−I battery, which has initial charging voltage of 3.60 V, the Li−I SFB achieves a voltage reduction of 0.70 V (3.60 − 2.90 = 0.70 V), which translates to energy savings of close to 20% (0.70 V/3.60 V × 100% = 19%). This charging voltage is even lower than the discharging voltage, which is thermodynamically impossible without the solar energy input.

As the charging process proceeds, the accumulation of I_3^- and consumption of I^- shifts the I_3^-/I^- redox potential positively and reduces the catholyte's ionic conductivity. Therefore, the charging voltages of both devices gradually increase due to the increasing internal resistance and the more-severe electrolyte−dye recombination (for the Li−I SFB case). At a cutoff voltage of 3.6 V, the solar battery with 0.100 mL of catholyte (2.00 M LiI, 0.50 M GuSCN in saturated Cheno aqueous solution) is able to be photocharged to a volumetric capacity of 32.6 Ah L^{-1} in 16.80 h, which is 91% of its theoretical capacity (i.e., 35.7 Ah L^{-1} for the catholyte with 2.00 M LiI). This value is close to the capacity of conventional Li−I batteries in the literature.[5b] Our Li−I SFB also demonstrates good cyclability. As shown in Figure 5b, the initial charging voltage remains stable at 2.91 ± 0.02 V for at least 25 cycles through continuous cycling. (See SI for experimental details and capacity calculations of Figure 5a,b.) Although the volumetric capacity of 35.7 Ah L^{-1} is promising for practical applications, it should be noted that the current system is limited by the low photocharging rate (i.e., 16.80 h per 0.1 mL catholyte). We attribute this to two factors: (1) the poor photocurrent performance of the dye-sensitized TiO_2 photoelectrode in an aqueous electrolyte and (2) the low Li^+-ionic conductivity of the ceramic membrane separator (i.e., up to 10^{-4} S cm^{-1} at room temperature). Thus, the application of more efficient aqueous compatible semiconductor photoelectrodes and the development of better ionic-conductive membrane are necessary for further improving the performance of the Li−I SFB system.

This Li−I SFB design also demonstrates efficient performance with an aprotic catholyte as well as the aqueous catholyte. Similar experiments were performed with a catholyte that used dimethyl sulfoxide (DMSO) as the solvent. The DMSO-based solar battery has a photoassisted charging voltage of 2.80 V under 1 sun 1.5 AM illumination and a discharging voltage of 3.32 V at the current density of 0.50 mA cm^{-2} (Figures S3−S5). Benefiting from its flow catholyte design, the Li−I SFB's operating power and cell capacity are decoupled. The maximum operating current/power depends on the area of the photoelectrode and electrolyte separator; while the cell's capacity is controlled by the amount of catholyte (assuming sufficient supply of the metallic Li anode). Therefore, the cell capacity can be designed such that the solar illumination time can match the photocharging time under specific operating conditions.

Furthermore, this concept can serve as a more generic design for extension to other metal based SFBs. The rich photoelectrochemistry of liquid-junction solar cells[12] and recent research efforts on metal-redox flow batteries[5,9,13] make it possible to explore other suitable combinations between redox couples and photoelectrodes for efficient SFBs. For instance, choosing a semiconductor with a more negative CBM (e.g., GaP) than TiO_2 as the photoelectrode can further reduce the required photocharging voltage. Meanwhile, applying a redox couple with a more positive redox potential (e.g., Br_2/Br^-) as the catholyte could help increase the output discharging voltage. A combination of these two approaches will enhance the solar energy saving efficiency. It is also worth exploring alternative anode materials to replace the metallic lithium anode. In particular, the sodium-based SFB presents unique advantages because of its richer supply of anode raw material, cheaper fabrication costs, and wider choices for Na^+ ion-conductive membrane materials. In fact, our preliminary tests on a sodium−iodine based system (Na−I SFB) have clearly demonstrated such feasibility (Figures S6 and S7). Research on developing other SFB systems is currently ongoing.

In conclusion, we have demonstrated the concept of an aqueous Li−I solar flow battery, which integrates a Li−I battery and a DSC into a single device, allowing for simultaneous solar energy conversion and storage. The photoassisted charging process allows this device to achieve energy savings close to 20%. Because it uses a metallic Li anode and aqueous catholyte, this Li−I SFB not only works with a higher output voltage (>3 V) but also is more environmentally friendly and cost-effective. Furthermore, this work's concept of combining battery electrochemistry with solar cell photoelectrochemistry also serves as a guiding design that can be extended to other metal−redox flow battery systems.

■ ASSOCIATED CONTENT

Supporting Information

Experimental details, discussion on CV of aqueous and aprotic catholyte based Li−I SFB, molecular structure of Z907 dye, results of DMSO-based Li−I SFB, and results of Na−I SFB. The

DOI: 10.1021/jacs.5b03626
J. Am. Chem. Soc. 2015, 137, 8332−8335

Supporting Information is available free of charge on the ACS Publications website at DOI: 10.1021/jacs.5b03626.

AUTHOR INFORMATION

Corresponding Author

*wu@chemistry.ohio-state.edu

Notes

The authors declare no competing financial interest.

ACKNOWLEDGMENTS

We acknowledge funding support from the U.S. Department of Energy, Office of Basic Energy Sciences, Division of Materials Science and Engineering (Award: DE-FG02-07ER46427). We thank B. B. Trang for her detailed and valuable comments on the manuscript.

REFERENCES

(1) (a) Gray, H. B. *Nat. Chem.* **2009**, *1*, 7. (b) Magnuson, A.; Anderlund, M.; Johansson, O.; Lindblad, P.; Lomoth, R.; Polivka, T.; Ott, S.; Stensjö, K.; Styring, S.; Sundström, V. *Acc. Chem. Res.* **2009**, *42*, 1899−1909,. (c) Schlapbach, L.; Zuttel, A. *Nature* **2001**, *414*, 353−358,. (d) Alibabaei, L.; Luo, H. L.; House, R. L.; Hoertz, P. G.; Lopez, R.; Meyer, T. J. *J. Mater. Chem. A* **2013**, *1*, 4133−4145,. (e) Khaselev, O.; Turner, J. A. *Science* **1998**, *280*, 425−427,. (f) Maeda, K.; Teramura, K.; Lu, D.; Takata, T.; Saito, N.; Inoue, Y.; Domen, K. *Nature* **2006**, *440*, 295−295,.

(2) (a) Chen, T.; Qiu, L.; Yang, Z.; Cai, Z.; Ren, J.; Li, H.; Lin, H.; Sun, X.; Peng, H. *Angew. Chem., Int. Ed.* **2012**, *51*, 11977−11980,. (b) Guo, W.; Xue, X.; Wang, S.; Lin, C.; Wang, Z. L. *Nano Lett.* **2012**, *12*, 2520−2523,. (c) Fu, Y.; Wu, H.; Ye, S.; Cai, X.; Yu, X.; Hou, S.; Kafafy, H.; Zou, D. *Energy Environ. Sci.* **2013**, *6*, 805−812,. (d) Yu, M.; Ren, X.; Ma, L.; Wu, Y. *Nat. Commun.* **2014**, *5*, 5111. (e) Hauch, A.; Georg, A.; Krašovec, U. O.; Orel, B. *J. Electrochem. Soc.* **2002**, *149*, A1208−A1211,. (f) Nagai, H.; Segawa, H. *Chem. Commun.* **2004**, *8*, 974−975,. (g) Murakami, T. N.; Kawashima, N.; Miyasaka, T. *Chem. Commun.* **2005**, *26*, 3346−3348,. (h) Chen, H.-W.; Hsu, C.-Y.; Chen, J.-G.; Lee, K.-M.; Wang, C.-C.; Huang, K.-C.; Ho, K.-C. *J. Power Sources* **2010**, *195*, 6225−6231,. (i) Saito, Y.; Uchida, S.; Kubo, T.; Segawa, H. *Thin Solid Films* **2010**, *518*, 3033−3036,. (j) Wee, G.; Salim, T.; Lam, Y. M.; Mhaisalkar, S. G.; Srinivasan, M. *Energy Environ. Sci.* **2011**, *4*, 413−416,.

(3) (a) Yan, N. F.; Li, G. R.; Gao, X. P. *J. Mater. Chem. A* **2013**, *1*, 7012−7015,. (b) Yan, N. F.; Li, G. R.; Gao, X. P. *J. Electrochem. Soc.* **2014**, *161*, A736−A741,. (c) Liu, P.; Cao, Y.-l.; Li, G.-R.; Gao, X.-P.; Ai, X.-P.; Yang, H.-X. *ChemSusChem* **2013**, *6*, 802−806,.

(4) (a) Wei, Z.; Liu, D.; Hsu, C.; Liu, F. *Electrochem. Commun.* **2014**, *45*, 79−82,. (b) Liu, D.; Wei, Z.; Hsu, C.-j.; Shen, Y.; Liu, F. *Electrochim. Acta* **2014**, *136*, 435−441,. (c) Liu, D.; Zi, W.; Sajjad, S. D.; Hsu, C.; Shen, Y.; Wei, M.; Liu, F. *ACS Catal.* **2015**, *5*, 2632−2639,.

(5) (a) Zhao, Y.; Byon, H. R. *Adv. Energy Mater.* **2013**, *3*, 1630−1635,. (b) Zhao, Y.; Wang, L.; Byon, H. R. *Nat. Commun.* **2013**, *4*, 1896. (c) Zhao, Y.; Hong, M.; Bonnet Mercier, N.; Yu, G.; Choi, H. C.; Byon, H. R. *Nano Lett.* **2014**, *14*, 1085−1092,.

(6) O'Regan, B.; Gratzel, M. *Nature* **1991**, *353*, 737−740,.

(7) (a) Law, C.; Pathirana, S. C.; Li, X.; Anderson, A. Y.; Barnes, P. R. F.; Listorti, A.; Ghaddar, T. H.; O'Regan, B. C. *Adv. Mater.* **2010**, *22*, 4505−4509,. (b) Law, C.; Moudam, O.; Villarroya-Lidon, S.; O'Regan, B. *J. Mater. Chem.* **2012**, *22*, 23387−23394,.

(8) Dean, J. L. *Lange's Handbook of Chemistry*, 14th ed.; McGraw Hill: New York, 1992.

(9) Wang, Y.; He, P.; Zhou, H. *Adv.Energy Mater.* **2012**, *2*, 770−779,.

(10) Boschloo, G.; Hagfeldt, A. *Acc. Chem. Res.* **2009**, *42*, 1819−1826,.

(11) Wang, Q.; Ito, S.; Gratzel, M.; Fabregat-Santiago, F.; Mora-Sero, I.; Bisquert, J.; Bessho, T.; Imai, H. *J. Phys. Chem. B* **2006**, *110*, 25210−25221,.

(12) (a) Kamat, P. V.; Tvrdy, K.; Baker, D. R.; Radich, J. G. *Chem. Rev.* **2010**, *110*, 6664−6688,. (b) Gratzel, M. *Nature* **2001**, *414*, 338−344,.

(13) (a) Lu, Y.; Goodenough, J. B.; Kim, Y. *J. Am. Chem. Soc.* **2011**, *133*, 5756−5759,. (b) Wang, Y.; Wang, Y.; Zhou, H. *ChemSusChem* **2011**, *4*, 1087−1090,. (c) Zhao, Y.; Ding, Y.; Song, J.; Li, G.; Dong, G.; Goodenough, J. B.; Yu, G. *Angew. Chem., Int. Ed.* **2014**, *53*, 11036−11040,. (d) Zhao, Y.; Ding, Y.; Song, J.; Peng, L.; Goodenough, J. B.; Yu, G. *Energy Environ. Sci.* **2014**, *7*, 1990−1995,. (e) Lu, Y.; Goodenough, J. B. *J. Mater. Chem.* **2011**, *21*, 10113−10117,. (f) Li, N.; Weng, Z.; Wang, Y.; Li, F.; Cheng, H.-M.; Zhou, H. *Energy Environ. Sci.* **2014**, *7*, 3307−3312,.

DOI: 10.1021/jacs.5b03626
J. Am. Chem. Soc. 2015, 137, 8332−8335